


Ultrafast quantum path interferometry to determine the electronic decoherence time of the electron-phonon coupled system in *n*-type gallium arsenide

Itsuki Takagi ^{1,2,*}, Yosuke Kayanuma,^{1,3} and Kazutaka G. Nakamura^{1,2,†}

¹Laboratory for Materials and Structures, Institute of Innovative Research, Tokyo Institute of Technology, 4259 Nagatsuta, Yokohama 226-8503, Japan

²Department of Materials Science and Engineering, Tokyo Institute of Technology, 4259 Nagatsuta, Yokohama 226-8503, Japan

³Graduate School of Sciences, Osaka Metropolitan University, 1-1 Gakuen-cho, Sakai, Osaka 599-8531, Japan



(Received 13 January 2023; revised 5 April 2023; accepted 26 April 2023; published 11 May 2023)

Quantum coherence is the key to new quantum technologies, although the details of decoherence processes and times are still not well understood in solids. We demonstrate how to measure the decoherence time of electronic excited states in *n*-type gallium arsenide (*n*-GaAs) crystals using a relative-phase locked double pulse excitation method and quantitatively evaluate with a simple model including temperature dependence. The interference patterns of both electronic and phonon coherence are observed in *n*-GaAs using ultrafast quantum path interferometry with $\pi/4$ polarized femtosecond pulses, via the amplitude of longitudinal optical phonons as a function of pump-pump delay. The electronic coherence shows uplifting and splitting in the collapse and revival of the electronic interference, which is sensitive to temperature, and these features are well reproduced using a simple quantum mechanical model. The decoherence time is determined using quantum calculations, from the splitting and uplifting in the interference shape, to be 27.8 ± 0.5 , 23.0 ± 0.3 , and 12.9 ± 0.3 fs at 10, 90, and 290 K, respectively. The temperature dependence of the decoherence time is well reproduced by the density of electrons in the conduction band with the group velocity of the photoinduced electrons.

DOI: [10.1103/PhysRevB.107.184305](https://doi.org/10.1103/PhysRevB.107.184305)

I. INTRODUCTION

Quantum coherence represents a superposition of quantum states and has been widely studied in atomic [1], molecular [2], biological [3,4], and solid-state systems [5–9]. In solid-state materials, any coherence disappears quickly due to interactions with the environment, and consequently the decoherence time and mechanism are still not well understood.

Optical phonons are often coherently induced by irradiating a crystal lattice with ultrashort optical pulses [10–15]. These can be observed using a pump-probe method in time-resolved reflection or transmission measurements [16–20]; often called coherent optical phonons, they are a superposition of phonon Fock states that can be interpreted as a coherence of phonon states. During the photoexcitation process, the wave packets of quantum superpositions are generated via several quantum transition pathways and evolution of phonon coherence can be evaluated via the decay of coherent oscillation in transient reflection or transmission. By using double-pump pulses, the generated wave packets undergo quantum interference with each other [21–23]. These quantum interferences can be manipulated by controlling the polarization and the delay time between double pulses, which is called coherent control [24–27]. Furthermore, by applying a relative phase of the optical pulses, not only phonon interference but also electronic interference can be observed [28,29].

In our previous work, we have performed quantum path interferometry to study the quantum coherence of the electron-phonon coupled system in *n*-type gallium arsenide (*n*-GaAs) single crystals using femtosecond pulses with relative phase locking [29,30]. Under the parallel polarization of double-pump pulses, both electronic coherence with rapid oscillation (~ 2.7 fs period) and phononic interference with slow oscillation (~ 115 fs period) can be simultaneously observed. Electronic coherence is also found to have a longer lifetime than the optical interference and also shows collapse-revival behavior [29]. In contrast, with orthogonal polarization, only phononic interference is observed in this situation, with no electronic interference being observed [30].

This interference behavior can be theoretically explained using a simple quantum mechanical model, consisting of two electronic bands and a single longitudinal optical (LO) phonon mode, with a classical optical electric field and the Raman tensor [29,31]. Theory predicts that uplifting and splitting will be observable in the collapse and revival of the electronic interference, when the two pump pulses are at $\pi/4$ relative polarization. Moreover, this characteristic uplift and splitting width is sensitively dependent on the decoherence in *n*-GaAs. This allows decoherence time to be determined quantitatively from the values of the height and width in the interference pattern.

In this study, we demonstrate quantitative determination of the electronic decoherence time in the electron-phonon coupled system (*n*-GaAs), using ultrafast quantum path interferometry experiments with relative-phase locking and $\pi/4$ polarization. Temperature dependence of the electronic decoherence time is also discussed.

*Corresponding author: takagi.i.aa@m.titech.ac.jp

†Corresponding author: nakamura@msl.titech.ac.jp

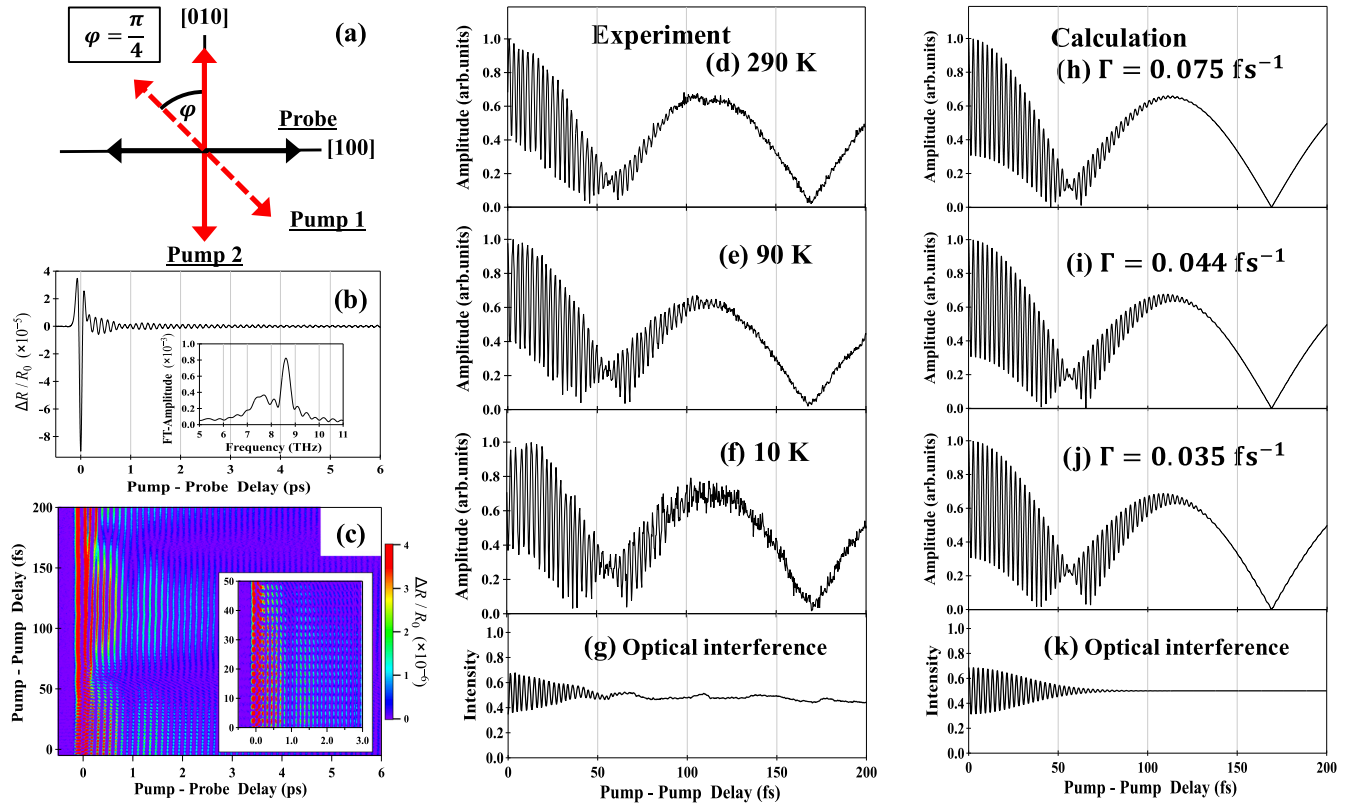


FIG. 1. Quantum path interferometry on the n -GaAs (001) surface. (a) The relation between the electric polarization of pump 1, pump 2, and probe pulse and the crystal orientation ([100] and [010]). The red dotted and solid lines show the electric polarization of pump 1 and pump 2, respectively. The black solid line shows electric polarization of the probe pulse. φ is the angle between the polarization of pumps 1 and 2, set to $\pi/4$. (b) Pump-probe delay dependence of the relative change in transient reflectivity ($\Delta R/R_0$) in double-pulse excitation at pump-pump delay time (t_{12}) of approximately 0 fs under 290 K. (c) Two-dimensional image map of the change in transient reflectance intensity with pump-probe delay and pump-pump delay, under the $\pi/4$ relative polarized pump pulse condition, at 290 K. (d)–(g) Measured LO phonon amplitudes as a function of pump-pump delay time t_{12} at (d) 290 K, (e) 90 K, (f) 10 K, and (g) optical interference of pump pulses. (h)–(k) The calculated LO phonon amplitudes as a function of pump-pump delay time at a relative polarization angle of $\pi/4$ for the parameter Γ : (h) 0.075 fs^{-1} , (i) 0.044 fs^{-1} , (j) 0.035 fs^{-1} , and (k) theoretical optical interference of pump pulses. Each calculated result reflects the experimental visibility of optical interference. The vertical axis is normalized by the maximum phonon amplitude of all data in experiment and theory.

II. EXPERIMENT

Using a pump-probe method with double-pump pulses, we measure the transient reflectance from the (001) plane in a single crystal of n -type GaAs with a thickness of 0.35 mm. The sample is doped with Si at a donor concentration of $1.0 \times 10^{18} \text{ cm}^{-3}$ and set in a cryostat.

This experimental setup [29] uses a Ti:sapphire laser (KM laser), producing pulses of width ~ 60 fs at a repetition rate of 94 MHz centered at approximately 800 nm. Chirped mirrors compensate for the dispersion in group velocity of the optics. A beam splitter divides the pulse into pump and probe pulses. The pump pulse is directed into a scan delay driven at 20 Hz to control the pump-probe delay (t_{13}) and a custom built Michelson-type interferometer to create double-pump pulses. In this interferometer, we use a feedback stage (Sigma Tech Co. Ltd.) in the optical path of pump 2 to control the pump-pump time delay (t_{12}) in steps of 300 attoseconds. A wave plate ($\lambda/2$) and a linear polarizer placed in each optical path set the polarization direction and optical intensity, before a lens focuses the pump and probe pulses onto the n -GaAs crystal in the cryostat. A portion of the double-pump pulses

created by the Michelson-type interferometer is extracted by a beam sampler and introduced into the optical monitor system. With this system, interference between pump pulses is also observed simultaneously during transient reflectance measurements.

Applying the electro-optic (EO) sampling technique, photodetectors are used to measure the photocurrent of the reflected probe pulse. In this technique, a polarizing beam splitter separates the reflected probe pulse into a pair of beams, which are subsequently detected using twin balanced photodetectors. The differential signal detected in balanced photodetectors is amplified using a low-noise current amplifier and recorded using a digital oscilloscope. The signals are averaged 4000 times using an oscilloscope to remove electrical noise.

In this experiment, we set the relative polarized angle of the double-pump pulses to $\pi/4$. The pump pulse pairs were polarized in the crystal orientations $[-110]$ and $[010]$, respectively [Fig. 1(a)], with both intensities set to 10 mW. In addition, the probe pulse is polarized in the $[100]$ direction [Fig. 1(a)], with an intensity of 5 mW. To measure temperature dependence, three cryostat settings are used, at 290 K, 90 K, and 10 K.

III. EXPERIMENTAL RESULTS

Figure 1(b) shows the transient reflectance ($\Delta R/R_0$) obtained by double-pump pulse excitation ($t_{12} \approx 0$ fs) of the *n*-GaAs sample as a function of pump-probe delay (t_{13}) at 290 K with the light intensity of about 30 mW. A nonoscillation background signal was removed. After Fourier transformation with pump-probe delays ranging from 0.3 to 3.0 ps, the Fourier-transformed (FT) signals are approximately 7.6 THz and 8.6 THz. These correspond to oscillations of the longitudinal optical phonon-plasmon couple (LOPC) and LO phonon mode [14,15,32–34], where the LOPC mode is smaller than that of the LO phonons. The ratio of the LO and LOPC peaks in the Fourier spectrum depends on the range of the Fourier transform and results from the much shorter lifetime of the LOPC mode compared to the LO phonons. Therefore, we focus only on the LO phonon in this study.

Figure 1(c) shows two-dimensional image maps of the relative change in transient reflection ($\Delta R/R_0$) against pump-probe delay (t_{13}) and pump-pump delay (t_{12}). We vary t_{12} in steps of 300 attoseconds and measure the transient reflectance of each pump-pump delay. At a delay time t_{12} between pump pulses, we observe two types of oscillations: (1) slow oscillation with a period of approximately 115 fs, corresponding to the LO phonon of GaAs, and (2) rapid oscillation with a period of approximately 2.7 fs.

To see greater detail of the interference behavior at a pump-pump delay time of (t_{12}), Fourier transforms are performed for all pump-pump data along with the pump-probe delay [e.g., horizontal axis in Fig. 1(b)]. Subsequently, we plot the 8.6 THz signal corresponding to the LO phonon signal versus the pump-pump delay time. Figure 1(d) shows rapid oscillation via electronic coherence simultaneously with slow interference fringes due to phononic interference. Moreover, electronic coherence is confirmed to persist for a longer time than optical interference. The splitting width of the electronic interference is 15.9 ± 0.3 fs. We observe a less pronounced amplitude suppression in the interference shape near the pump-pump delay time $t_{12} = 0$ fs, which is different to our previously reported results under parallel polarization [29].

Figures 1(d)–1(f) show the measured LO phonon amplitudes (i.e., interference of quantum coherence) as a function of pump-pump delay time t_{12} at 290 K, 90 K, and 10 K conditions. The electronic decoherence time increases at lower temperatures. By focusing on the quantum coherence's interference shape at a pump-pump delay time around $t_{12} = 55$ fs, a significant triangle pattern (due to uplifting of the phonon amplitude and splitting of the interference shape) is observed with decreasing temperature. This uplifting of the phonon amplitude is a characteristic phenomenon caused by quantum path interference in the impulsive stimulated Raman scattering (ISRS) process [29]. Notably, this splitting width is seen to expand as the temperature decreases, with the splitting widths of the electronic interference at 10 and 90 K obtained to be 27.4 and 24.6 ± 0.3 fs, respectively. Note that we define splitting value as the width of the triangles observed in the quantum interference shape when the pump-pump delay t_{12} is around 55 fs. Furthermore, we define the experimental and theoretical uplifting value as the height from the minimum phonon amplitude to the point of the electronic interference

collapse-revival behavior. Details of the definition of uplifting and splitting are given in the Supplemental Material [35].

IV. THEORETICAL CALCULATION

The theoretical model for the coherent control of LO phonons in GaAs by double-pulse excitation is derived using the quantum mechanical model and ISRS process [31], described as follows. This model was derived using a simplified electronic band model, the phonon state as a harmonic oscillator, and the electron-phonon interaction taking into account the allowed and forbidden Raman scattering process [20,36–38]. The Hamiltonian model and calculation of the density operator corresponding to the double-sided Feynman diagrams are described in detail elsewhere [31] and in the Supplemental Material [35]. In this model, the resonant excitation occurs at an energy slightly higher than the excitation band edge of GaAs and coherent phonons are generated. We therefore introduce a phenomenological effective response function $F(t)$ to describe the probability of electron transition to the energy region corresponding to resonant Raman scattering. In this calculation, we use a simplified Lorenz model for the effective response function

$$F(t) = \sum_k |\mu_k|^2 e^{-\frac{i}{\hbar}(\epsilon_k - \epsilon_g)t - \eta|t|/\hbar} \quad (\eta = 0_+),$$

$$= |\mu|^2 \exp(-i\Omega_c t - \Gamma|t|), \quad (1)$$

where μ corresponds to the effective transition dipole moment, Ω_c to the center frequency of the optical pulse and Γ to the decay constant, which is the reciprocal of the electronic decoherence time.

We calculate the four quantum pathways in optical transition via ISRS with double-pump pulses. The visibility of optical interference in the experiment [Fig. 1(g)] is confirmed to be only approximately 75% of perfect interference (100%), so we therefore consider a contribution of 0.75 from the two quantum pathways related to electronic coherence.

Figures 1(h)–1(j) show the calculated LO phonon amplitudes as a function of pump-pump delay time at a relative polarization angle of $\pi/4$ while varying the parameter Γ . In these figures, the theoretical results confirm that the experimental interference shapes are well reproduced. In particular, the splitting or uplifting of the interference shape shows a similar change as the decay constant Γ decreases, i.e., as the decoherence time increases, the feature interference pattern formed becomes more significant as in the case of the experimental lower temperature.

These results strongly suggest that the splitting and uplifting of the interference shape are dependent upon the decay constant. Moreover, it is possible to determine the decoherence time in electron-phonon coupled states by comparing the theoretical and experimental splitting widths and uplifting of phonon amplitudes, calculations of which, as a function of the decay constant, are shown in Fig. 2.

V. DISCUSSION

Using the calculated relation between the splitting width or uplifting of phonon amplitude and the decay constant (Fig. 2),

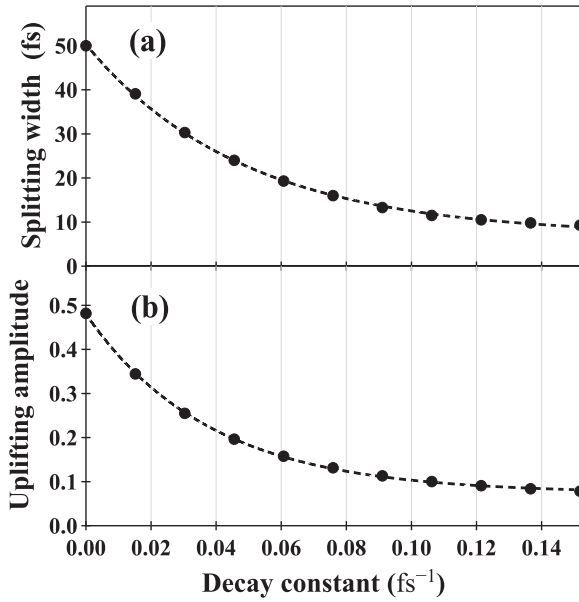


FIG. 2. Relation among the calculated decay constant Γ , the splitting width, and the uplifting of the phonon amplitude in the interference shapes at around $t_{12} = 55$ fs; (a) splitting width where the phonon amplitude reaches a minimum. (b) Uplifting amplitude at the moment of collapse and revival of the electronic coherence.

the electronic decoherence time at each temperature is obtained, shown in Fig. 3 with a plot of decoherence time as a function of temperature. Each decoherence time was determined by comparing experimental and theoretical splitting and uplifting values of triangle pattern in quantum interference shape. The electronic decoherence time is found to be

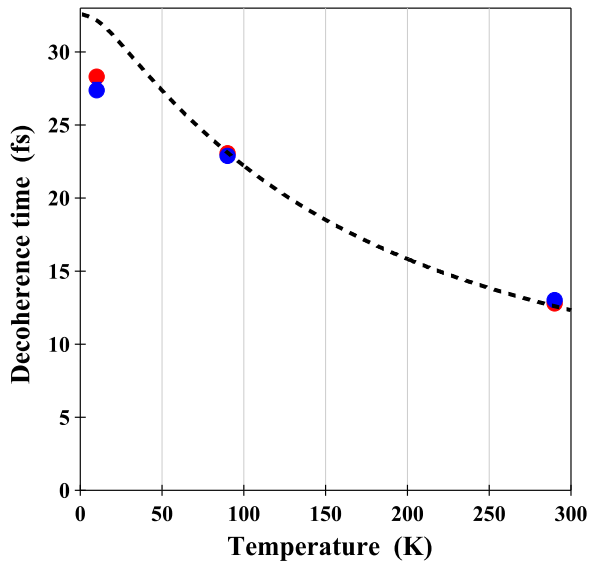


FIG. 3. Decoherence time as a function of temperature. The red and blue dotted lines show experimental decoherence times obtained by uplifting of phonon amplitude and splitting width, respectively. The black dashed line is the relation between the electronic decoherence time and temperature estimated by the quantum kinetic theory [Eq. (3)].

27.8 ± 0.5 , 23.0 ± 0.3 , and 12.9 ± 0.3 fs at each temperature of 10, 90, and 290 K, decreasing as the temperature increases, respectively.

Wegener *et al.* [7,8,43,44] have studied the influence of photoinduced carriers on electronic coherence in bulk GaAs (0.6 μm layer in GaAs/Al_{0.3}Ga_{0.7}As) using four-wave mixing (FWM) and photon-echo techniques at room temperature. They report that the electronic decoherence time (τ) is 18 fs at a carrier density of 10^{17} cm^{-3} and is dependent on the photoexcited carrier density n_e as

$$\tau^{-1} = \tau_0^{-1} + c n_e^{1/3}, \quad (2)$$

where n_e is the sum of the two individual photoexcited carrier densities ($n_e = n_{e1} + n_{e2}$), τ_0 is the decay constant for scattering by phonons, and $\tau_0 = 100$ fs. The coefficient c can be estimated from Fig. 1 in Ref. [7] to be $9 \times 10^7 \text{ cm/s}$.

In this study, two types of carriers may contribute to electronic coherence. One is the photoinduced carriers under irradiation by double-pump pulses, while the other is the carrier density from Si dopants. It is necessary to consider the contribution of both carrier densities to the theoretical model in Eq. (2).

In Eq. (2), the parameter τ_0 is the decay constant for scattering by phonons and c is the coefficient. Here, we consider the meaning of parameter c . Examination of the unit dimension of Eq. (2) shows that the first terms on the left and right sides are in $1/\text{s}$. For the second term on the right side, $n_e^{1/3}$ has a unit in cm^{-1} . We infer the dimension of c to be cm/s and interpreted as akin to the group velocity of electrons. Calculating the group velocity of electrons excited by the optical pulse (1.55 eV) using the free electron model ($E = \hbar^2 k^2 / 2m_n + E_c$) at 300 K gives an estimated group velocity $8.4 \times 10^7 \text{ cm/s}$.

Subsequently, we attempt to evaluate the decoherence time due to the photoinduced and dopant carrier densities by using the modified quantum kinetic theory in Eq. (2) as

$$\tau^{-1} = \tau_0^{-1} + v(T)[n_d(T) + n_e(T)]^{1/3}, \quad (3)$$

where $\tau_0 = 100$ fs, $v(T)$ is the group velocity of electrons, and $n_d(T)$ is the dopant carrier density. $n_e(T)$ is the photoinduced carrier density with double-pump pulses, which was derived using the pulse power at maximum interference. Details of each carrier density are given in the Supplemental Material [35]. The estimated decoherence time with respect to temperature is shown in Fig. 3, in which the estimated values are shown to agree well with the experimental results. Equation (3) can be easily interpreted as follows. $[n_d(T) + n_e(T)]^{1/3}$ corresponds to the reciprocal of the mean distance between electrons in the conduction band. $v(T)$ corresponds to the group velocity of the photoinduced electron in the conduction band. Consequently, $v(T) \times [n_d(T) + n_e(T)]^{1/3}$ corresponds to the reciprocal of the collision time. Therefore, the decoherence time can be determined by the collision time for the photoexcited electrons in the conduction band in the present condition. The experimentally obtained decoherence time at 10 K is shorter than the estimated values and there are two possible explanations for this. One is that the free electron model may not explain the parameter value of $v(T)$ at extremely low temperatures, because the band structure and effective mass change with temperature. Alternatively, τ_0 may depend on temperature because the lifetime caused by

phonon scattering, such as electron-phonon scattering, varies with temperature. In actuality, the estimated decoherence time becomes lower and more consistent with the experimental decoherence time at 10 K when τ_0 is set to a time shorter than 100 fs. In addition, excitons are generated by electrons at the conduction band edge as the temperature decreases. Consequently, the carrier density is expected to decrease and the electronic decoherence time should increase beyond the estimated time in this calculation. However, our experimental result shows a shorter decoherence time at 10 K. This may be due to the fact that our observations concern electronic coherence at energies beyond the band edge, which are relatively less affected by exciton generation. Further experiments with various pump power densities, center wavelengths, and temperatures will help to further elucidate the details of the decoherence mechanism.

VI. CONCLUSION

We investigate the electronic decoherence time in the electron-phonon coupled system (*n*-GaAs) using ultrafast quantum path interferometry experiments with relative-phase locked and $\pi/4$ -polarized double-pulse excitation. The

decoherence time is quantitatively determined from the uplifing of phonon amplitude and the split width is obtained with the help of a quantum mechanical model calculation: 27.8 ± 0.5 , 23.0 ± 0.3 , and 12.9 ± 0.3 fs at 10, 90, and 290 K. The temperature dependence of the decoherence time is discussed from the perspective of electron density and is reproduced using carrier densities in the conduction band and the group velocity of the photoinduced electrons. The derived formulas with electronic dispersion, photon energy, and intensity will be expected to evaluate the electronic decoherence time in solids. We also anticipate that the ultrafast quantum path interferometry will be used to examine quantitatively electronic and phononic decoherence times in solids.

ACKNOWLEDGMENTS

We thank M. Suda, R. Takai, and M. Hirose for their help with the experiments. This work was partially supported by JSPS KAKENHI under Grants No. 19K03696, No. 19K22141, No. 21H04669, No. 21K18904, No. 22J23231, No. 22H01984, and No. 22KJ1342, and by Design & Engineering by Joint Inverse Innovation for Materials Architecture, MEXT.

-
- [1] I. Bloch, Quantum coherence and entanglement with ultracold atoms in optical lattices, *Nature (London)* **453**, 1016 (2008).
 - [2] K. Bader, D. Dengler, S. Lenz, B. Endeward, S. D. Jiang, P. Neugebauer, and J. Slageren, Room temperature quantum coherence in a potential molecular qubit, *Nat. Commun.* **5**, 5304 (2014).
 - [3] S. Lloyd, Quantum coherence in biological systems, *J. Phys.: Conf. Ser.* **302**, 012037 (2011).
 - [4] N. Lambert, Y. Chen, Y. C. Cheng, C. M. Li, G. Y. Chen, and F. Nori, Quantum biology, *Nat. Phys.* **9**, 10 (2013).
 - [5] W. W. Chow, H. C. Schneider, and M. C. Phillips, Theory of quantum-coherence phenomena in semiconductor quantum dots, *Phys. Rev. A* **68**, 053802 (2003).
 - [6] S. Welinski, P. J. T. Woodburn, N. Lauk, R. L. Cone, C. Simon, P. Goldner, and C. W. Thiel, Electron Spin Coherence in Optically Excited States of Rare-Earth Ions for Microwave to Optical Quantum Transducers, *Phys. Rev. Lett.* **122**, 247401 (2019).
 - [7] W. A. Hügel, M. F. Heinrich, M. Wegener, Q. T. Vu, L. Bányai, and H. Haug, Photon Echoes from Semiconductor Band-to-Band Continuum Transitions in the Regime of Coulomb Quantum Kinetics, *Phys. Rev. Lett.* **83**, 3313 (1999).
 - [8] M. Wegener, Quantum coherence in semiconductors, *J. Lumin.* **87-89**, 20 (2000).
 - [9] M. U. Wehner, M. H. Ulm, D. S. Chemla, and M. Wegener, Coherent Control of Electron-LO-Phonon Scattering in Bulk GaAs, *Phys. Rev. Lett.* **80**, 1992 (1998).
 - [10] Y. X. Yan, E. B. Gamble, Jr., and K. Nelson, Impulsive stimulated scattering: General importance in femtosecond laser pulse interactions with matter, and spectroscopic applications, *J. Chem. Phys.* **83**, 5391 (1985).
 - [11] R. Merlin, Generating coherent THz phonons with light pulses, *Solid State Commun.* **102**, 207 (1997).
 - [12] H. J. Zeiger, J. Vidal, T. K. Cheng, E. P. Ippen, G. Dresselhaus, and M. S. Dresselhaus, Theory for displacive excitation of coherent phonons, *Phys. Rev. B* **45**, 768 (1992).
 - [13] A. V. Kuznetsov and C. J. Stanton, Theory of Coherent Phonon Oscillations in Semiconductors, *Phys. Rev. Lett.* **73**, 3243 (1994).
 - [14] T. Dekorsy, G. C. Cho, and H. Kurz, in *Light Scattering in Solids VIII*, edited by M. Cardona and G. Guntherodt (Springer, Berlin, 2000), pp. 169–209.
 - [15] G. C. Cho, W. Kutt, and H. Kurz, Subpicosecond Time-Resolved Coherent-Phonon Oscillations in GaAs, *Phys. Rev. Lett.* **65**, 764 (1990).
 - [16] K. Sokolowski-Tinten, C. Blome, J. Blums, A. Cavalleri, C. Dietrich, A. Tarasevitch, I. Uschmann, E. Förster, M. Kammler, M. Horn-von-Hoegen, and D. von der Linde, Femtosecond X-ray measurement of coherent lattice vibrations near the Lindemann stability limit, *Nature (London)* **422**, 287 (2003).
 - [17] S. L. Johnson, P. Beaud, C. J. Milne, F. S. Krasniqi, E. S. Zijlstra, M. E. Garcia, M. Kaiser, D. Grolimund, R. Abela, and G. Ingold, Nanoscale Depth-Resolved Coherent Femtosecond Motion in Laser-Excited Bismuth, *Phys. Rev. Lett.* **100**, 155501 (2008).
 - [18] R. P. Chatelain, V. R. Morrison, B. L. M. Klarenaar, and B. J. Siwick, Coherent and Incoherent Electron-Phonon Coupling in Graphite Observed with Radio-Frequency Compressed Ultrafast Electron Diffraction, *Phys. Rev. Lett.* **113**, 235502 (2014).
 - [19] T. Dekorsy, T. Pfeifer, W. Kutt, and H. Kurz, Subpicosecond carrier transport in GaAs surface-space-charge fields, *Phys. Rev. B* **47**, 3842 (1993).
 - [20] T. Pfeifer, T. Dekorsy, W. Kütt, and H. Kurz, Generation mechanism for coherent LO phonons in surface-space-charge fields of III-V-compounds, *Appl. Phys. A* **55**, 482 (1992).

- [21] D. J. Tannor and S. A. Rice, Control of selectivity of chemical reaction via control of wave packet evolution, *J. Chem. Phys.* **83**, 5013 (1985).
- [22] P. Brumer and M. Shapiro, Control of unimolecular reactions using coherent light, *Chem. Phys. Lett.* **126**, 541 (1986).
- [23] D. J. Tannor, R. Kosloff, and R. A. Rice, Coherent pulse sequence induced control of selectivity of reactions: Exact quantum mechanical calculations, *J. Chem. Phys.* **85**, 5805 (1986).
- [24] H. Katsuki, N. Takei, C. Sommer, and K. Ohmori, Ultrafast coherent control of condensed matter with attosecond precision, *Acc. Chem. Res.* **51**, 1174 (2018).
- [25] H. Mashiko, Y. Chisuga, I. Katayama, K. Oguri, H. Masuda, J. Takeda, and H. Gotoh, Multi-petahertz electron interference in Cr : Al₂O₃ solid-state material, *Nat. Commun.* **9**, 1468 (2018).
- [26] T. Kimata, K. Yoda, H. Matsumoto, H. Tanabe, F. Minami, Y. Kayanuma, and K. G. Nakamura, Coherent control of 40-THz optical phonons in diamond using femtosecond optical pulses, *Phys. Rev. B* **101**, 174301 (2020).
- [27] I. Takagi, T. Kato, Y. Kayanuma, and K. G. Nakamura, Interference of optical phonons in diamond studied using femtosecond pulses of polarized near-infrared light, *Solid State Commun.* **350**, 114747 (2022).
- [28] S. Hayashi, K. Kato, K. Norimatsu, M. Hada, Y. Kayanuma, and K. G. Nakamura, Measuring quantum coherence in bulk solids using dual phase-locked optical pulses, *Sci. Rep.* **4**, 4456 (2014).
- [29] K. G. Nakamura, K. Yokota, Y. Okuda, R. Kase, T. Kitashima, Y. Mishima, Y. Shikano, and Y. Kayanuma, Ultrafast quantum-path interferometry revealing the generation process of coherent phonons, *Phys. Rev. B* **99**, 180301(R) (2019).
- [30] H. Matsumoto, T. Kitashima, T. Maruhashi, I. Takagi, Y. Kayanuma, and K. G. Nakamura, Coherent control of optical phonons in GaAs by relative-phase-locked optical pulses under perpendicularly polarized conditions, *Solid State Commun.* **327**, 114215 (2021).
- [31] I. Takagi, Y. Kayanuma, and K. G. Nakamura, Theory for coherent control of longitudinal optical phonons in GaAs using polarized optical pulses with relative phase locking, *Phys. Rev. B* **104**, 134301 (2021).
- [32] A. Mooradian and A. L. McWhorter, Polarization and Intensity of Raman Scattering from Plasmons and Phonons in Gallium Arsenide, *Phys. Rev. Lett.* **19**, 849 (1967).
- [33] J. D. Lee and M. Hase, Coherent Optical Control of the Ultrafast Dephasing of Phonon-Plasmon Coupling in a Polar Semiconductor Using a Pulse Train of Below-Band-Gap Excitation, *Phys. Rev. Lett.* **101**, 235501 (2008).
- [34] J. Hu, O. V. Misochnko, A. Goto, and K. G. Nakamura, Delayed formation of coherent LO phonon-plasmon coupled modes in *n*- and *p*-type GaAs measured using a femtosecond coherent control technique, *Phys. Rev. B* **86**, 235145 (2012).
- [35] See Supplemental Material at <http://link.aps.org/supplemental/10.1103/PhysRevB.107.184305> for the details of definitions of uplifting and splitting of a quantum path interference, theoretical model, calculations of doped carrier density, laser intensity and estimated photoinduced carrier density, and estimated decoherence times for photoexcited electrons from heavy and light holes, which includes Refs. [31,36–42].
- [36] K. Ishioka, A. K. Basak, and H. Petek, Allowed and forbidden Raman scattering mechanisms for detection of coherent LO phonon and plasmon-coupled modes in GaAs, *Phys. Rev. B* **84**, 235202 (2011).
- [37] C. Trallero-Giner, A. Cantarero, and M. Cardona, One-phonon resonant Raman scattering: Fröhlich exciton-phonon interaction, *Phys. Rev. B* **40**, 4030 (1989).
- [38] P. Y. Yu and M. Cardona, *Fundamentals of Semiconductors: Physics and Materials Properties*, 3rd ed. (Springer, New York, 2001), pp. 378–394.
- [39] S. M. Sze, Y. Li, and K. K. Ng, *Physics of Semiconductor Devices*, 4th ed. (Wiley, New York, 2021).
- [40] J. S. Blakemore, Semiconducting and other major properties of gallium arsenide, *J. Appl. Phys.* **53**, R123 (1982).
- [41] E. Vigil, J. A. Rodríguez, and R. Pérez Alvarez, Optical constants of *n*- and *p*-type GaAs between 2.5 and 3.5 eV, *Phys. Status Solidi B* **90**, 409 (1978).
- [42] M. D. Sturge, Optical Absorption of Gallium Arsenide between 0.6 and 2.75 eV, *Phys. Rev.* **127**, 768 (1962).
- [43] H. Haug and J.-P. Jauho, in *Quantum Kinetics in Transport and Optics of Semiconductors*, 2nd substantially revised ed., Springer Series in Solid-State Sciences, Vol. 123 (Springer-Verlag, Berlin, 2008), and references therein.
- [44] W. Schäfer and M. Wegener, *Semiconductor Optics and Transport Phenomena* (Springer-Verlag, Berlin, 2002).